

# Optimal Design for Thermodynamic System with OpenModelica and MATLAB/Simulink

Kazuki Yoshida<sup>1</sup> Hitoi Ono<sup>1</sup> Hirotaka Okazaki<sup>1</sup>

<sup>1</sup> Mitsubishi Heavy Industries, Ltd., Japan, {kazuki.yoshida.ws, hitoi.ono.x3, hirotaka.okazaki.hy}@mhi.com

## Abstract

The complicated thermodynamic system includes nonlinear characteristics and is expressed by high order differential algebraic equations. Therefore, it is difficult to carry out numerical analysis such as optimization. To deal with this problem, we verify an integrated design support environment incorporating OpenModelica for a centrifugal chiller as an example. In this paper, it is shown that the parameters of the model and the control logic can be adjusted by the coupled simulation of the chiller model written in the Modelica language and the control logic on MATLAB/Simulink. We also simplify the centrifugal chiller model by approximating the nonlinear characteristics with a smooth polynomial, and by reducing the order of the differential algebraic equation by the Pantelides method. Then, a case study of a startup profile optimization is shown.

*Keywords:* thermodynamic system, optimization, design tool, FMI

## 1 Introduction

There is an increasing demand for efficient operation of energy equipment for the transition to a carbon-free society. In order to develop and commercialize a device composed of a wide variety of equipment in a short time, it is important to use dynamic simulation in the early stage of development, and determine the feasibility including operation characteristics. In general, this dynamic simulation uses a precise model close to the actual machine. However, in performing a mathematical optimization in order to adjust model parameters based on actual machine data or to generate an operation profile, a smooth approximate model suitable for optimization is required. These approximation models were developed manually and took time.

In this study, an integrated design support environment incorporating OpenModelica is verified using a centrifugal chiller as an example. Figure 1 shows the environment's work flows and main 3 features, (1) Profile optimization, (2) Logic verification and (3) Software-In-the-Loop-Simulation (SILS) verification.

First, a detailed dynamic model of the chiller is developed in the Modelica language (Fritzson, 2004). This model and a control logic are coupled with MATLAB/Simulink. With this coupling calculation, (1) Vali-

dation of control logic, (2) Fitting model parameters by mathematical optimization, and (3) Optimization of control parameters are possible. Either the control logic defined by MATLAB/Simulink or the execution file of control logic for real machine (regardless of programming language) can be used. The latter is SILS verification. In the optimization of the control parameters, optimization may be performed to match the optimal profile (described later) and the state variables of coupling simulation. This paper shows a parameter optimization without using an optimal profile.

Next, in performing profile optimization, simplified models, in which the nonlinear characteristics are approximated by a smooth polynomial, are prepared. Further, since the combined whole system model becomes a high-order differential algebraic equation (DAE) having two or more differential exponents, a mathematical processing of reducing the order is applied. Then, simplified model is exported as XML format by OpenModelica (Shitahun et al., 2013). The profile optimization problem for chiller startup is formulated from this XML file by using collocation method (Sabbagh and Gómez, 2018). Next, this problem is converted into Python script, which can be treated by optimization modeling tool CasADi (Andersson et al., 2012). Finally, optimized profile is calculated by CasADi and nonlinear programming (NLP) solver IPOPT (Wächter and Biegler, 2006)

The remainder of this paper is structured as follows: The configuration and model of the turbo chiller, and the simulation by Modelica are shown in Section 2. In Section 3, we present the tuning of equipment parameters and control parameters by using the coupled calculations on MATLAB/Simulink. Section 4 describes profile optimization using an approximate model. Section 5 shows a summary and future perspective.

## 2 Centrifugal chiller dynamic model

### 2.1 Process

As shown in Figure 2, the centrifugal chiller has two heat exchangers (evaporator, condenser) and a gas-water separator (economizer), and a two-stage centrifugal compressor and three valves (high-stage expansion valve, low-stage expansion valve, and hot gas bypass valve) (Okazaki et al., 2022). The non-CFC (Chlorofluorocar-

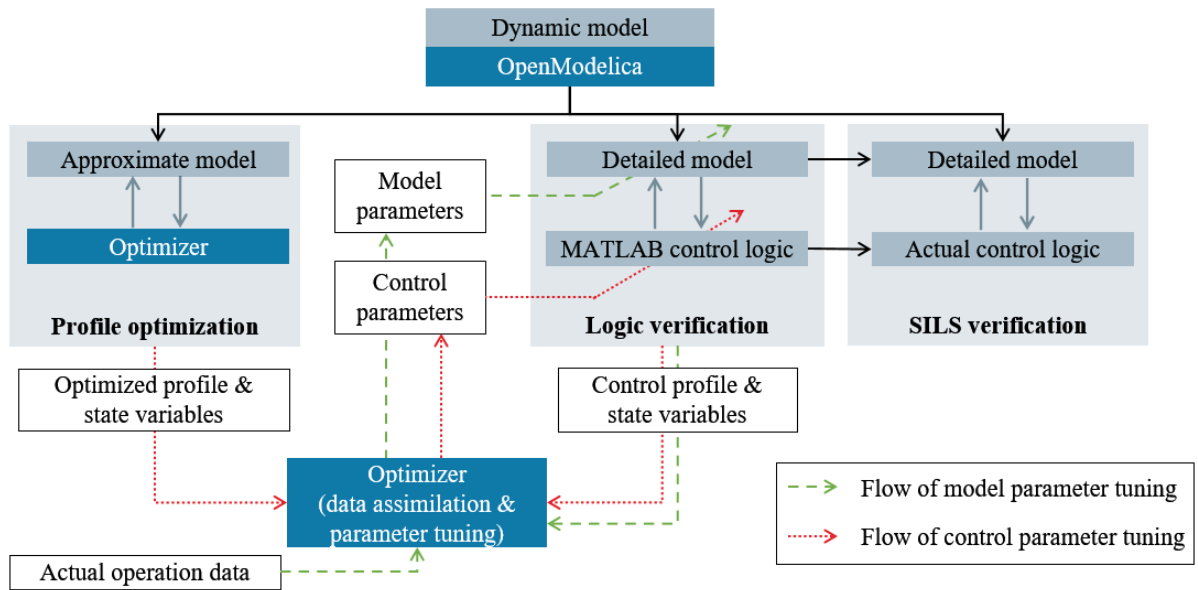


Figure 1. Work flows and features of the integrated design support environment

bon) type refrigerant circulating in the centrifugal chiller evaporates by heat exchange with chilled water in the evaporator and is sucked into the 1st stage compressor. The refrigerant adiabatically compressed by the two-stage compressor maintains the gas phase state and flows into the condenser. In the condenser, the refrigerant condenses by removing heat with cooling water. The refrigerant in the liquid phase state is depressurized by the high stage expansion valve, and a part of the refrigerant is vaporized. The vaporized refrigerant is separated from the liquid phase by the economizer and sucked into the middle stage of the compressor, and the liquid phase is further depressurized by the low stage expansion valve and flows into the evaporator. Chilled water that has been cooled to 7°C by being deprived of heat by the refrigerant in the evaporator is supplied to the HVAC (Heating Ventilation and Air Conditioning) system. By cooling the air conditioning air, the chilled water raises itself 12°C and returns to the evaporator. The cooling water rises to 37°C after it is used to cool the refrigerant in the condenser. In the cooling tower, the temperature is lowered to 32°C by a heat exchanger with air and returned to the condenser. The control of the centrifugal chiller is to maintain the chilled water outlet temperature at the set value temperature of 7°C against fluctuations in the cooling load, and the rotation speed of the compressor is manipulated. Furthermore, in order to operate the centrifugal chiller at a higher efficiency point, the vane opening of the two-stage compressor and the opening of the high stage expansion valve and the low stage expansion valve are manipulated to adjust the refrigerant circulation flow rate. The hot gas bypass valve is used to avoid a surge in the compressor by opening it at a low flow rate such as when starting up or when the load is low.

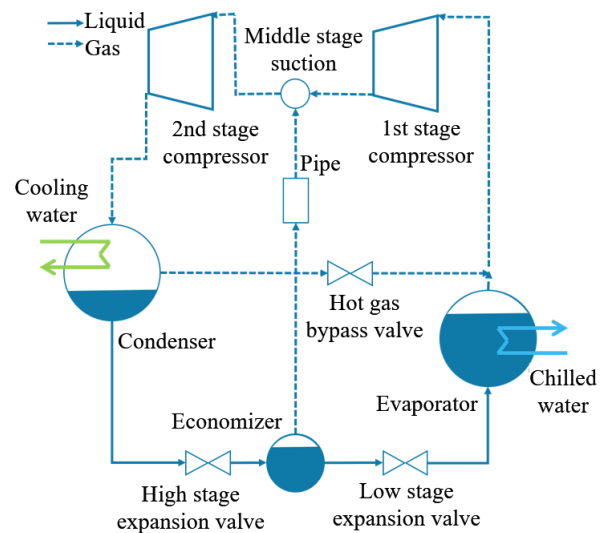


Figure 2. Configuration of centrifugal chiller

## 2.2 Physical models

Among the equipment constituting the centrifugal chiller, the evaporator, the condenser, and the economizer have a liquid level, and the refrigerant is in a two-phase state. In this study, it is assumed that the refrigerants in these devices are saturated, and the mass balance and energy balance are considered by the following Equation 1 and 2. Here,  $\rho$  ( $\text{kg}/\text{m}^3$ ) is the average density of the liquid phase and the gas phase in the device, and  $E$  ( $\text{kJ}/\text{m}^3$ ) is the average energy density.  $V$  ( $\text{m}^3$ ) is a volume of equipment,  $G$  ( $\text{kg}/\text{sec}$ ) is a mass flow rate, and  $h$  ( $\text{kJ}/\text{kg}$ ) indicates specific enthalpy. Subscript letters in and out indicate inflow and outflow to the equipment.  $Q$  ( $\text{kJ}/\text{sec}$ ) indicates the amount of heat for cold water, cooling water and re-

refrigerant in the evaporator or condenser (Bendapudi et al., 2002).

$$V \cdot \frac{dp}{dt} = (G_{in} - G_{out}) \quad (1)$$

$$V \cdot \frac{dE}{dt} = (G_{in} \cdot h_{in} - G_{out} \cdot h_{out} + Q) \quad (2)$$

$\rho$  and  $E$  are expressed according to Equation 3 and 4 using void fraction  $\beta$ , the density and the enthalpy of the liquid phase and the gas phase in the saturation state. Subscript letters l and g indicate liquid and gas phase.

$$\rho = \beta \cdot \rho_g + (1 - \beta) \cdot \rho_l \quad (3)$$

$$E = \beta \cdot \rho_g \cdot h_g + (1 - \beta) \cdot \rho_l \cdot h_l \quad (4)$$

When  $\beta$  is erased from these two equations,  $\rho$  and  $E$  are represented by the following Equation 5. Since  $\rho_g$ ,  $\rho_l$ ,  $h_g$ , and  $h_l$  can be approximated by a polynomial of pressure  $P$  (MPa), it is possible to obtain  $P$  and  $\beta$  from  $\rho$  and  $E$ , which are independent variables.

$$E = \frac{(\rho_g \cdot h_g - \rho_l \cdot h_l)}{(\rho_g - \rho_l)} \cdot \rho + \frac{(\rho_g \cdot \rho_l \cdot h_l - \rho_l \cdot \rho_g \cdot h_g)}{(\rho_g - \rho_l)} \quad (5)$$

The chilled water outlet temperature  $T_{weo}$  ( $^{\circ}\text{C}$ ) and the cooling water outlet temperature  $T_{wco}$  can be calculated from the following energy balance Equation 6 and 7 using the amount of heat exchange in the evaporator  $Q_e$  (kJ/sec) and condenser  $Q_c$ , respectively. Here,  $H_e$  and  $H_c$  indicate the heat capacity of the metal of the heat transfer tube and chilled and cooling water in the tube.  $G_{we}$  (kg/sec) and  $G_{wc}$  are the chilled water flow rate and the cooling water flow rate, and  $cp_{we}$  (kJ/kg/ $^{\circ}\text{C}$ ) and  $cp_{wc}$  are the specific heat respectively.

$$H_e \cdot \frac{dT_{weo}}{dt} = G_{we} \cdot cp_{we} \cdot (T_{wei} - T_{weo}) + Q_e \quad (6)$$

$$H_c \cdot \frac{dT_{wco}}{dt} = G_{wc} \cdot cp_{wc} \cdot (T_{wci} - T_{wco}) - Q_c \quad (7)$$

$Q_e$  and  $Q_c$  are calculated by the following Equation 8 and 9 from the chilled water input  $T_{wei}$ , output temperature, the cooling water input  $T_{wci}$ , output temperature, evaporation temperature  $T_e$ , condensation temperature  $T_c$ , and heat transfer performance  $UA_e$  (kJ/sec/ $^{\circ}\text{C}$ ) and  $UA_c$ .  $f_e$  and  $f_c$  are functions for calculating the temperature difference between the refrigerant, chilled water, and cooling water.

$$Q_e = UA_e \cdot f_e(T_{wei}, T_{weo}, T_e) \quad (8)$$

$$Q_c = UA_c \cdot f_c(T_{wci}, T_{wco}, T_c) \quad (9)$$

The mass flow rate  $G_{cpj}$  passing through each stage of the compressor is calculated from the differential pressure

$\Delta P_{cpj}$  (MPa) at the inlet and outlet, the specific volume  $v_{cpj}$  ( $\text{m}^3/\text{kg}$ ), the rotation speed  $N_{cp}$  (%), the vane opening degree  $V_{cpj}$  (%), and the flow rate characteristic map  $f_{cpj}$  of the compressor by Equation 10.

$$G_{cpj} = f_{cpj}(\Delta P_{cpj}, v_{cpj}, N_{cp}, V_{cpj}) \quad (10)$$

The mass flow rate  $G_{ev}$  through the expansion valve is calculated from the differential pressure  $\Delta P_{ev}$  at the inlet and outlet, the elevation difference  $\Delta L_{ev}$  (MPa), the specific volume  $v_{ev}$ , the expansion valve opening  $V_{ev}$ , and the CV value determined from the CV characteristics  $f_{ev}$  by Equation 11.

$$G_{ev} = \frac{f_{ev}(V_{ev})}{v_{ev}} \sqrt{\Delta P_{ev} + \Delta L_{ev}} \quad (11)$$

The mass flow rate  $G_{by}$  through the bypass valve is calculated from the condensation pressure  $P_c$ , evaporation pressure  $P_e$ , the specific volume  $v_c$ , the bypass valve opening  $V_{by}$ , and the CV characteristics  $f_{by}$  by Equation 12.

$$G_{by} = \frac{f_{by}(V_{by})}{v_c} \sqrt{P_c^2 - P_e^2} \quad (12)$$

The outlet enthalpy of the compressor  $h_{cpoj}$  is calculated by the following Equation 13 and 14 from the inlet enthalpy  $h_{cpij}$ , the value assuming the isentropic change  $h_{cpoj}^{id}$ , and the efficiency determined  $\eta_{cpj}$  from the compressor characteristics  $f_{cpj}$  (Bendapudi and Braun, 2002).

$$h_{cpoj} = h_{cpoj} + \frac{(h_{cpoj}^{id} - h_{cpoj})}{\eta_{cpj}} \quad (13)$$

$$\eta_{cpj} = f_{cpj}(\Delta P_{cpj}, N_{cp}, V_{cpj}) \quad (14)$$

### 2.3 Approximation of non-linear characteristics

In general, since the pressure loss is proportional to the square of the flow rate, the relationship between the differential pressure  $\Delta P$  and the flow rate  $G$  is expressed as bellow (Okazaki et al., 2022).

$$G \propto \text{sign}(\Delta P) \sqrt{|\Delta P|} \quad (15)$$

It is hard to optimize with Equation 15 since the slope of the right-hand side of the expression is  $\infty$  when  $\Delta P$  is 0. So, we represent Equation 15 to as bellow, firstly. The square root calculation is replaced by ReLU function. The ReLU function returns 0 when a negative value is an argument, or returns the input value if a positive value is an argument (Glorot et al., 2011).

$$\text{sign}(\Delta P)\sqrt{|\Delta P|} = \sqrt{\text{ReLU}(\Delta P)} - \sqrt{\text{ReLU}(-\Delta P)} \quad (16)$$

The entire square root function is represented as a smooth curve, Equation 18, by replacing the ReLU function with the Softplus function of Equation 17.

$$\text{Softplus}(x) = \frac{\log(1 + e^{kx})}{k} \quad (17)$$

$$\begin{aligned} \text{sign}(\Delta P)\sqrt{|\Delta P|} &\approx \sqrt{\text{Softplus}(\Delta P)} - \sqrt{\text{Softplus}(-\Delta P)} \\ &= \frac{\sqrt{\log(1 + e^{k\Delta P})} - \sqrt{\log(1 + e^{-k\Delta P})}}{\sqrt{k}} \end{aligned} \quad (18)$$

$k$  is a value greater than 0 and is a parameter which has trade-off between the approximation accuracy of the function and the smoothness of the approximation function. Secondly, an approximation method for upper and lower limit processing of values such as state variables is described below. At the boundary where the upper and lower limit processing is performed, the gradient becomes discontinuous and the second order differentiation becomes impossible. The function that limits  $x$  to the upper and lower bounds in the  $[L_x, U_x]$  interval can be written as follows.

$$\min(\max(x, L_x), U_x) = -\max(-\max(x, L_x), U_x) \quad (19)$$

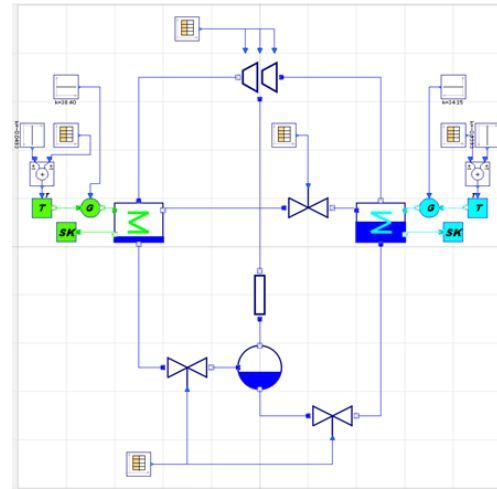
By replacing  $\max$  in Equation 19 with LSE (Log-Sum-Exp) of Equation 20, it can be expressed in Equation 21 (Nielsen and Sun, 2016).

$$\text{LSE}_k(x_1, \dots, x_n) = \frac{1}{k} \log(e^{kx_1} + \dots + e^{kx_n}) \quad (20)$$

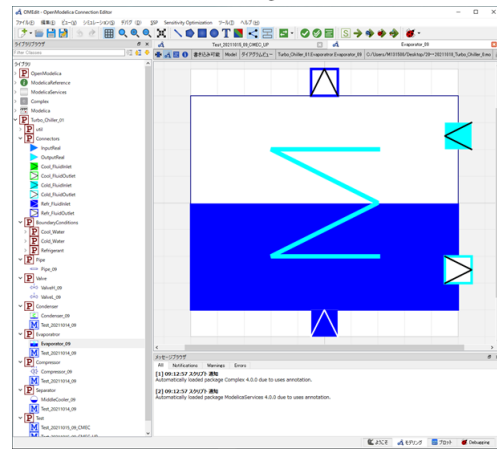
$$\begin{aligned} \min(\max(x, L_x), U_x) &= -\max(-\max(x, L_x), -U_x) \\ &= -\text{LSE}(-\text{LSE}(x, L_x), -U_x) \\ &= -\frac{1}{k} \log\left(\frac{1}{e^{kx} + e^{kL_x}} + e^{-kU_x}\right) \end{aligned} \quad (21)$$

Finally, we will describe that a model representing the backward enthalpy of this centrifugal chiller system can be expressed using a sigmoid function. This system may allow refrigerant to flow back, in which case the enthalpy flow must also be considered. It is necessary to switch the characteristics according to the direction in which the flow of the refrigerant. However, and the slope is discontinuous at the boundary of the switch. Thus, the representing characteristic switching model is expressed with Equation 22.

$$\text{sigmoid}(x) = \frac{1}{1 + e^{-kx}} \quad (22)$$



(a) Centrifugal chiller



(b) Evaporator

Figure 3. Models on OpenModelica

## 2.4 Validation

We implement the model of the centrifugal chiller in the previous section in Modelica language, and verify the model accuracy. The centrifugal chiller model on OpenModelica is shown in Figure 3(a). Considering deployment to chillers with different configurations, we implement each component. Figure 3(b) shows the evaporator component, which has the inlet and outlet to be connected to other components. Next, the components were combined in OpenModelica's GUI editor (OMedit) to build a model of the entire chiller. The entire model takes as input the number of revolutions of the compressor, the opening of the bypass valve, the coolant inlet temperature, etc. The numbers of differential equations and algebraic equations are 9 and 100, respectively.

Next, we execute the startup simulation, giving the same conditions of the actual machine, such as the inlet temperature and flow rate of chilled water and cooling water, and the command value from the control logic, as boundary conditions. The simulation results and the measurement results of the actual machine are shown in Figure 4. The normalized time on the horizontal axis of

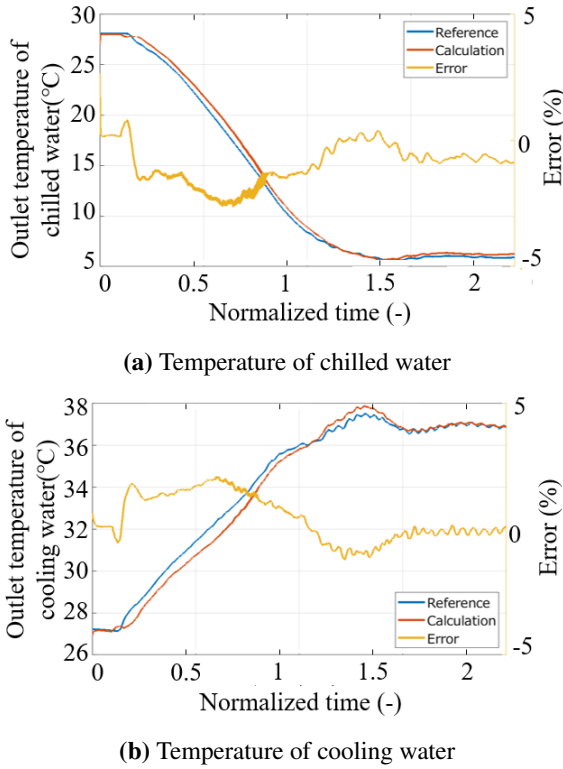


Figure 4. Validation results of centrifugal chiller model

the graphs represent the operation start point as 1. (In all the of following figures, the scaling factor is equal to that of Figure 4.) Both errors in the outlet temperature of chilled water and cooling water are within  $\pm 2.5\%$ . When the simulation period is 1800 seconds, the calculation time is 13.6 seconds (compilation: 12.0 seconds, and simulation: 1.6 seconds) with Intel Core i7-8700 CPU with 16 GB RAM machine.

### 3 Parameter tuning by coupled calculation

In this section, we describe how to perform coupled calculation of the model in Modelica language and the control logic on MATLAB/Simulink. Next, we present an example in which the parameters of the model are tuned to match the behavior of model to that of the actual machine. Finally, an example of optimizing the parameters of the control logic is shown.

#### 3.1 Coupling of chiller dynamic model and control logic

The construction of coupled calculation using MATLAB/Simulink is shown. The model of centrifugal chiller is exported in FMU format by OpenModelica. We use a executable file of the control logic. Next, the FMU file of the centrifugal chiller is imported in the FMU block of Simulink of the MATLAB R2019b. The control logic communicates with S-function block of Simulink. The simulation is performed while the centrifugal chiller

model and the control logic synchronize the time.

#### 3.2 Tuning of equipment parameters

The procedure for adjusting the equipment parameters is as follows: (1) Startup simulation is performed, while the same inputs from control logic as the actual machine test is given to the centrifugal chiller model. (2) The equipment parameters are optimized to minimize the error between the simulation results and the results of real machine tests.

We tried the adjustment of each heat transmission coefficient of condenser and evaporator. The evaluation function is as follows:

$$\text{minimize } \int (|P_c - \hat{P}_c| + |P_e - \hat{P}_e|) dt \quad (23)$$

Here,  $P_c$  and  $P_e$  are the pressure of condenser and the pressure of evaporator in the real machine test, respectively. Also,  $\hat{P}_c$  and  $\hat{P}_e$  are the pressure of condenser and the pressure of evaporator in the simulation, respectively. That is, heat transmission coefficients are optimized to minimize the pressure errors. The Bayesian optimization algorithm is used.

We use the Bayesian optimization algorithm (Shahriari et al., 2016) because it is difficult to calculate the gradient of the evaluation function. In this algorithm, a response surface is generated by Gaussian process regression from the sampled data. The response surface represents the predictive uncertainty, and then the next sampling point is determined while considering the balance between the exploration of the high uncertainty region and the exploitation of already obtained optimal solution.

After 800 optimization iterations, we obtain the heat transmission coefficients that reduce the evaluation function from 4.16 to 0.64. Figure 5(a) compares condenser pressures of actual machine and these of before and after tuning. Figure 5(b) also compares these of evaporator pressure. The pressure errors of these 2 equipments are reduced after optimization. The optimization time is 1280 seconds.

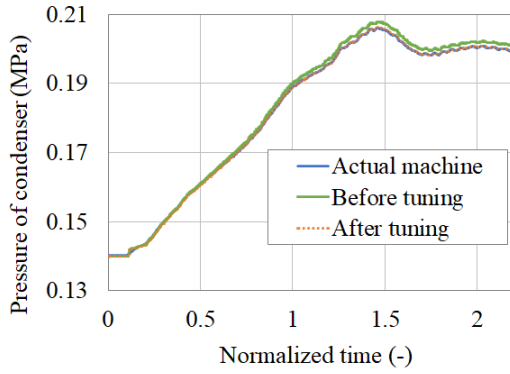
#### 3.3 Tuning of control parameters

We optimize the parameters of the control logic by using the coupled simulation to reduce the startup time of the centrifugal chiller. We choose 12 parameters, which have a large effect on the startup time. The evaluation function is the difference between the chilled water outlet temperature  $T_{wco}$  and the target temperature  $T_{wco,ref}$  as follows:

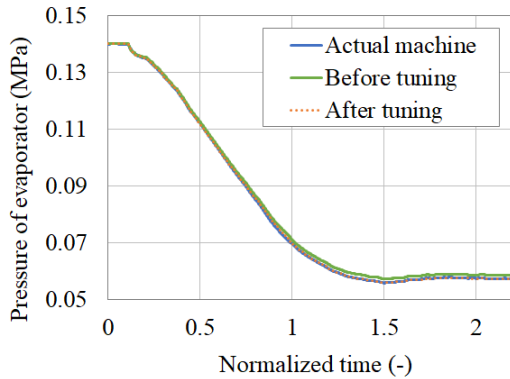
$$\text{minimize } \int |T_{wco} - T_{wco,ref}| dt \quad (24)$$

Here,  $T_{wco,ref}$  was set at 7 °C. The Bayesian optimization algorithm is used.

After 40 optimization iterations, the parameters to reduce startup time were obtained. The simulation results

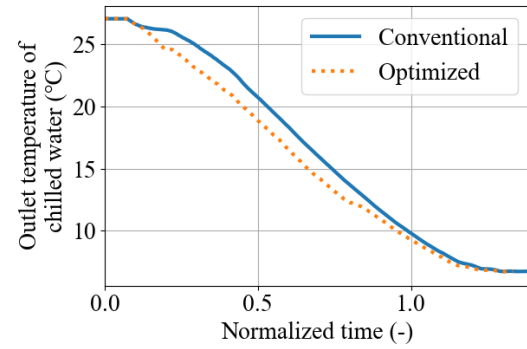


(a) Pressure of condenser

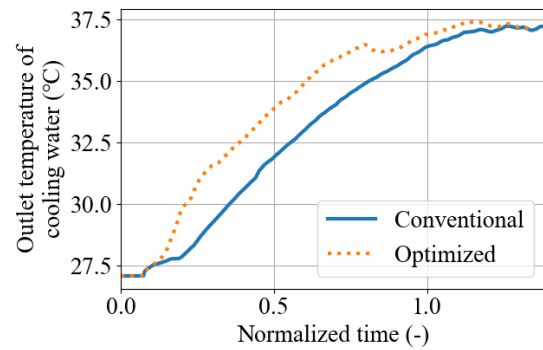


(b) Pressure of evaporator

Figure 5. Simulation results by tuned equipment parameters



(a) Temperature of chilled water



(b) Temperature of cooling water

Figure 6. Simulation results by tuned controller parameters

using the parameters before and after the optimization are shown in Figure 6. After the optimization, the outlet temperature of chilled water decreases faster to target value.

## 4 Dynamic optimization by approximation model

### 4.1 Approximation of non-linear characteristics

To improve convergence and reduce calculation time of complex dynamic system optimization, it is effective to approximate nonlinear characteristics with smooth polynomials. Therefore, we create approximate models, for example, property tables, pressure losses in valve and pipe (calculation of square root), operation ranges in valve and compressor (upper and lower limit), and evaluation of contraflow (if statement).

A model composed of multiple dynamic equipment generally has high-order DAE, whose order is 2 or more. On such complex models is difficult to perform numerical analysis such as simulation and optimization. In this study, we use the Pantelides method implemented in OpenModelica to reduce order of the model.

### 4.2 Formulation

We formulated the dynamic optimization as follows, where  $\mathbf{u}^i \in \mathbb{R}^{n_u}$  are the manipulated variables at time phase

$i$ : The rotation speed of the compressor, the vane opening of the two-stage compressors, the opening of the high stage expansion valve, and the low stage expansion valve at the boundary of each phase.  $n_u$  is the number of operation variables ( $n_u = 5$ ).  $\mathbf{x}^{i,j} \in \mathbb{R}^{n_x}$  indicate the state variables: The outlet temperature of the chilled water ( $T_{wco}$ ) or the cooling water ( $T_{wco}$ ), the density of the liquid phase or the gas phase of the evaporator ( $\rho_e$ ), the condenser ( $\rho_c$ ) or economizer ( $\rho_m$ ). The enthalpy of the liquid phase or the gas phase of the evaporator ( $E_e$ ), the condenser ( $E_c$ ) or economizer ( $E_m$ ) and pressure of the middle stage of the suction are also state variables.  $n_x$  is the number of state variables ( $n_x = 9$ ).  $\mathbf{z}^{i,j} \in \mathbb{R}^{n_z}$  are the algebraic variables: The pressure ( $P_c, P_e, P_m$ ), temperature ( $T_c, T_e, T_m$ ), liquid levels, and the mass flow rates of the condenser, evaporator and economizer. The flow rates of gas in the two-stage centrifugal compressor ( $G_{cp1}, G_{cp2}$ ) and the flow rate of liquid in the valves (high-stage expansion valve ( $G_h$ ), low-stage expansion valve ( $G_l$ ), and hot gas bypass valve ( $G_m$ )), the flow rates of and the hot gas bypass valve ( $G_{by}$ ) are also algebraic variables.  $n_z$  is the number of algebraic variables ( $n_z = 18$ ).  $\mathbf{r}^0$  and  $\mathbf{r}^n$  indicate the constraints in the initial condition and the termination condition.  $\mathbf{F}$  is the functions related to differential equations,  $\mathbf{G}$  is the functions related to algebraic equations,  $\mathbf{H}$  is the inequality constraint.  $n$  is the number of divisions in the time direction about manipulated variables, and  $m$  is the

number of state variables and algebraic variables.  $i = 0$  means initial phase and  $i = n$  indicates terminal phase. In this report with direct collocation method, the number of optimization variables are 137,508 ( $u$ :2500,  $x$ :45008,  $z$ :90000), equality constraints are 135,508, and inequality constraints are 2,500.

$$\begin{aligned}
 & \underset{\mathbf{U}, \mathbf{X}, \mathbf{Z}}{\text{minimize}} && J(\mathbf{X}, \mathbf{U}) \\
 & \text{subject to} && \mathbf{r}^{0,0}(\mathbf{x}^{0,0}, \mathbf{u}^0, \mathbf{z}^{0,0}) = \mathbf{0} \\
 & && \mathbf{r}^{n,m}(\mathbf{x}^{n,m}, \mathbf{u}^n, \mathbf{z}^{n,m}) = \mathbf{0} \\
 & && \mathbf{x}^{i,j+1} = \mathbf{F}(\mathbf{x}^{i,j}, \mathbf{u}^i, \mathbf{z}^{i,j}) \cdot \Delta t \\
 & && \mathbf{z}^{i,j} = \mathbf{G}(\mathbf{x}^{i,j}, \mathbf{u}^i) \\
 & && \mathbf{H}(\mathbf{x}^{i,j}, \mathbf{u}^i, \mathbf{z}^{i,j}) \geq \mathbf{0} \\
 & && \mathbf{x}_{min}^{i,j} \leq \mathbf{x}^{i,j} \leq \mathbf{x}_{max}^{i,j} \\
 & && \mathbf{u}_{min}^i \leq \mathbf{u}^i \leq \mathbf{u}_{max}^i \\
 & && \mathbf{U} = [\mathbf{u}^{0T}, \dots, \mathbf{u}^{nT}]^T \\
 & && \mathbf{X} = [\mathbf{x}^{0,0T}, \dots, \mathbf{x}^{n,mT}]^T \\
 & && \mathbf{Z} = [\mathbf{z}^{0,0T}, \dots, \mathbf{z}^{n,mT}]^T \\
 & && \forall i = 0, \dots, n \\
 & && \forall j = 0, \dots, m
 \end{aligned} \tag{25}$$

The objective function  $J$  consists of state variables and manipulated variables: The integration of the temperature difference between chilled water temperature (state variable) and the target temperature of  $7^\circ\text{C}$  in this centrifugal chiller. The refrigerant circulation flow rate, liquid levels are also considered. In addition, the penalty for the control variables affects the objective function.

### 4.3 Optimized profile

We demonstrate the profile optimization of startup of centrifugal chiller by using OpenModelica and CasADi. OpenModelica can export a Modelica model as XML format. CasADi is an optimization modeling tool, which has Python, C++ and Octave/MATLAB interfaces.

Profile optimization was performed as follows: (1) Reduce the order of centrifugal chiller model by OpenModelica and export as XML file. (2) Convert the XML file into a Python script executable by CasADi. (3) Perform profile optimization with CasADi and NLP solver IPOPT.

The optimization algorithm is a quasi-Newton method implemented in IPOPT. CasADi automatically generate the derivatives, which is required for the quasi-Newton method. The Bayesian optimization used in the previous section is not suitable for the profile optimization because the calculation cost increases in the large optimization problem.

The chilled water temperatures of optimization results are shown in Figure 7. The black line is inlet temperature, which is boundary condition. The 3 orange lines are outlet temperature. The solid and dotted orange lines are the simulation results where the conventional and optimized

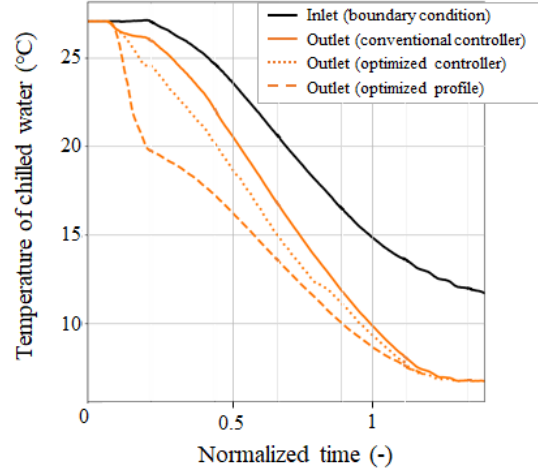


Figure 7. Temperature of chilled water by profile optimization

parameters of controller is used respectively. The dotted line, the optimized profile, shows the fastest decrease of outlet temperature, i.e., the fastest startup of the centrifugal chiller.

## 5 Conclusion

This paper presents a design support environment for thermodynamic systems. We conduct the coupled simulation on MATLAB/Simulink by using the chiller model in Modelica language and the control logic, and see that the parameters of the model and the control logic could be tuned. In addition, the startup profile optimization was carried out by the chiller model, which is simplified by smooth polynomial approximation and order reduction of DAE. Future work will focus on applying this design support environment to other cold products and chemical plants.

## References

- Joel Andersson, Johan Åkesson, and Moritz Diehl. Casadi: A symbolic package for automatic differentiation and optimal control. In *Lecture Notes in Computational Science and Engineering*, volume 87, 2012.
- Satyam Bendapudi and James E. Braun. A review of literature on dynamic models of vapor compression equipment. Report, ASHRAE Research project 1043-RP, 2002.
- Satyam Bendapudi, James E. Braun, and Eckhard A. Groll. A dynamic model of a vapor compression liquid chiller. In *International Refrigeration and Air Conditioning Conference. Paper 568*, 2002.
- Peter Fritzson. *Principles of Object Oriented Modeling and Simulation with Modelica 2.1*. Wiley-IEEE Press, 2004.
- Xavier Glorot, Antoine Bordes, and Yoshua Bengio. Deep sparse rectifier neural networks. In *Proceedings of the Fourteenth International Conference on Artificial Intelligence and Statistics*, volume 15 of *Proceedings of Machine Learning Research*, pages 315–323. PMLR, 2011.

- Frank Nielsen and Ke Sun. Guaranteed bounds on information-theoretic measures of univariate mixtures using piecewise log-sum-exp inequalities. *Entropy*, 18(12), 2016.
- Hiroataka Okazaki, Hitoi Ono, and Noritaka Yanai. Optimization of start-up operation for centrifugal chiller. In *18th IFAC Workshop "Control Applications of Optimization"*, 2022.
- Alejandro A. Sabbagh and Jorge M. Gómez. Optimal control of single stage liBr/water absorption chiller. *International Journal of Refrigeration*, 92:1–9, 2018.
- Bobak Shahriari, Kevin Swersky, Ziyu Wang, Ryan P. Adams, and Nando de Freitas. Taking the human out of the loop: A review of bayesian optimization. *Proceedings of the IEEE*, 104(1):148–175, 2016.
- Alachew Shitahun, Vitalij Ruge, Mahder Gebremedhin, Bernhard Bachmann, Lars Eriksson, Joel Andersson, Moritz Diehl, and Peter Fritzson. Model-based dynamic optimization with openmodelica and casadi. In *7th IFAC Symposium on Advances in Automotive Control*, pages 446–451, 2013.
- Andreas Wächter and Lorenz Biegler. On the implementation of an interior-point filter line-search algorithm for large-scale nonlinear programming. *Mathematical programming*, 106: 25–57, 2006.